The Astrophysical Journal Letters, 848:L3 (4pp), 2017 October 10 https://doi.org/10.3847/2041-8213/aa8def


# Origin of the Differential Fluxes of Low-energy Electrons in the Inner Heliosheath

H. J. Fahr[1], S. M. Krimigis[2,3], H. Fichtner[4], K. Scherer[4], A. Sylla[4], S. E. S. Ferreira[5], and M. S. Potgieter[5]
[1] Argelander Institut für Astronomie, Universität Bonn, Auf dem Hügel 71, 53121 Bonn, Germany; hf@tp4.rub.de
[2] Office of Space Research and Technology, Academy of Athens, 10679 Athens, Greece
[3] Applied Physics Laboratory, The Johns Hopkins University, Laurel, MD 20723, USA
[4] Institut für Theoretische Physik IV, Ruhr-Universität Bochum, 44780 Bochum, Germany
[5] Centre for Space Research, North-West University, 2520 Potchefstroom, South Africa
*Received 2017 September 4; accepted 2017 September 18; published 2017 October 4*

## Abstract

The study addresses the question of the origin of low-energy electrons measured by *Voyager 1* in the multi-keV range in the inner heliosheath. It intends to demonstrate that the observed keV-fluxes of electrons are consistent with their transmission through the termination shock under the influence of the associated electrostatic field. A power-law representation of the electron velocity distribution just downstream of the solar wind termination shock is motivated and formulated in terms of a so-called $\kappa$-distribution function. From this initial function spectral electron fluxes in the range 40–70 keV are derived and compared to the data. It is shown that with $\kappa$-values between 7 and 8 the data can be satisfactorily explained. Given these comparatively high $\kappa$-values, it is concluded that the electron distribution just downstream of the termination shock relaxes toward but does not reach a Maxwellian shape in the inner heliosheath.

*Key words:* acceleration of particles – methods: analytical – Sun: heliosphere

## 1. Introduction and Motivation

Beyond the solar wind termination shock energetic electrons in the energy interval 35–70 keV have been observed with the *Voyager 1* and *2* spacecraft (Decker et al. 2015); see also Figure 1 below. The *Voyager 1* observations suggest that these electrons, which appeared in this energy channel after the termination shock crossings, are of solar (wind) origin because their differential flux vanished again shortly before the heliopause crossing and remained absent in the local interstellar medium. From the latter observation one can conclude that they do not originate from interstellar cosmic electrons that were studied, e.g., by Langner et al. (2001) and recently by Prinsloo (2016) and Prinsloo et al. (2017). According to the estimates of the intensity of 100 keV Galactic electrons by Langner et al. (2001), the mentioned electron flux inside the heliosheath could be about $4 \cdot 10^3$ times higher than that in the local interstellar medium, so that an interstellar origin is considered improbable. Because the general features of these electrons are quite similar to those of the anomalous cosmic-ray component (see, e.g., Stone et al. 2013; Webber & McDonald 2013), they may be considered as anomalous electrons.

Energetic electrons in the range 1–35 keV in this distant space plasma region remain undetected and can, therefore, be classified as a neglected particle population. It is unlikely that this means that such electrons are absent: concerning theoretical studies it is usually assumed that the electron transition from upstream to downstream of the termination shock strictly obeys the Rankine–Hugoniot relations valid for the main momentum carrier, i.e., the ions. This means it is generally assumed that the electrons—regarding the properties of their moments—behave like the ions do, namely, attaining the same downstream densities, bulk velocities, and temperatures. Electrons and ions, however, cannot be assumed to be strongly bound to each other at such very localized shock structures: the locally very strong, shock-induced electric fields rather lead to a phenomenon called *spontaneous demagnetization* (see Lembège et al. 2003) due to which electrons in first order merely react to the shock-induced electric fields not recognizing any Lorentz forces. This behavior of electrons at shocks has been emphasized in recent papers by, e.g., Chalov & Fahr (2013) and Fahr et al. (2015). In particular, Fahr & Verscharen (2016) have demonstrated that, as a consequence of demagnetization, electrons gain high overshoot velocities at the solar wind termination shock corresponding to energies on the order of several keV. In the following, we demonstrate, by assuming as in Fahr & Siewert (2013) that the electron velocity distribution can be represented by a so-called $\kappa$-distribution, that the observed differential electron fluxes farther into the inner heliosheath can be consistently explained as a consequence of the electron behavior across the termination shock.

## 2. The Differential Electron Flux Model

### 2.1. The Distribution Function Downstream of the Termination Shock

Recently, Fahr & Verscharen (2016) have derived the electron distribution function immediately downstream of the shock region where electric forces are dominating Lorentz forces. Farther downstream the electrons have to adapt to the magnetic field, frozen into the downstream bulk solar wind ion flow, moving with the reduced ion bulk speed $U_1/s = U_2$, with the shock compression ratio $s$. Hence, the bulk of the downstream electrons moves with a speed $\boldsymbol{U} = \boldsymbol{U}_e - \boldsymbol{U}_2$ relative to the ions with components $U_{\parallel,\perp}$ along and perpendicular to the downstream magnetic field $\boldsymbol{B}_2$. Due to the Lorentz forces electrons are forced to form a torus distribution with an average velocity $U_\perp$ and a thermal spread of $\sqrt{3k_{\rm B}T_1/m_e}$ depending, according to Liouville's theorem, on the upstream electron temperature $T_1$, the Boltzmann constant $k_{\rm B}$, and the electron mass $m_e$. If the electrons are subject to fast pitch-angle scattering (see, e.g., Wykes et al. 2001), the initial toroidal

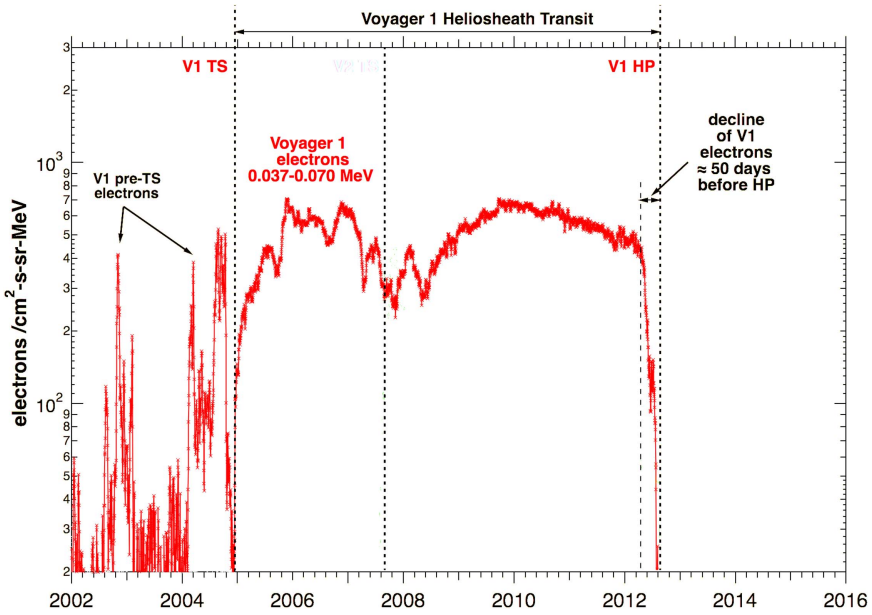


**Figure 1.** Differential flux $j_{\rm obs}$ of electrons in the energy interval 37–70 keV measured by *Voyager 1* in the inner heliosheath (Krimigis 2015).

distribution evolves into an isotropic shell distribution:

$$f_{\rm shell}(v) \propto n_e \exp\left[-\frac{m_e(v-U_\perp)^2}{k_{\rm B}T_{\rm l}}\right]. \quad (1)$$

As demonstrated by various authors (e.g., Isenberg 1987; Bogdan et al. 1991; Fahr & Fichtner 2011) this distribution rapidly evolves further into a quasi-stationary distribution, which we assume to be a $\kappa$-distribution (Fahr & Siewert 2013):

$$f_v(v) = \frac{n_e}{\pi^{3/2}U_\perp^3}\frac{\Gamma(\kappa+1)}{\kappa^{3/2}\Gamma(\kappa-1/2)}\left[1+\frac{v^2}{\kappa U_\perp^2}\right]^{-\kappa-1}, \quad (2)$$

where $n_e$ is the total electron number density, $U_\perp$ defines the core width, $\Gamma(x)$ denotes the Gamma function, and $\kappa$ is the index quantifying the "suprathemal deviation" from a Maxwellian, which is obtained in the limit $\kappa \to \infty$.

### 2.2. The Differential Electron Flux in the Inner Heliosheath

The differential flux (particles per area per time interval per solid angle and per energy interval) is given by $j(p) = p^2 f_p(p)$ with the momentum distribution $f_p(p)$ that is related to the velocity distribution via

$$f_p(p) = \frac{f_v(v)}{m_e^3} \quad (3)$$

where $m_e$ denotes the electron mass. In order to compare the model directly to data, the differential flux should be calculated in terms of energy using $E = (m_e v^2)/2 = p^2/(2m_e)$:

$$j(E) = p^2(E) f_p(p(E)) = \frac{2E}{m_e^2} f_v(v(E)). \quad (4)$$

With Equation (2), this yields

$$j(E) = \frac{2n_e E}{\pi^{3/2}m_e^2 U_\perp^3}\frac{\Gamma(\kappa+1)}{\kappa^{3/2}\Gamma(\kappa-1/2)}\left[1+\frac{2E}{\kappa m_e U_\perp^2}\right]^{-\kappa-1}, \quad (5)$$

which is consistent with the formula given in Hapgood et al. (2011). Upon introducing the (reference) energy $E_0 = U_\perp^2 m_e/2$ one obtains

$$j(E) = \frac{n_e E}{\sqrt{2\pi^3 m_e}E_0^{3/2}}\frac{\Gamma(\kappa+1)}{\kappa^{3/2}\Gamma(\kappa-1/2)}\left[1+\frac{E}{\kappa E_0}\right]^{-\kappa-1}. \quad (6)$$

## 3. Quantitative Comparison to Measurements

In order to check whether the observed differential electron flux can be explained with the shock-processed electrons, it has to be shown to be consistent with Equation (2) for reasonable parameter values.

A direct comparison of numerical results calculated with Equation (6) with measurements of the observed differential flux is required to integrate $j(E)$ over the interval $E_{\rm l} = 37$ keV to $E_2 = 70$ keV and to normalize it to $E_2 - E_{\rm l}$ so that

$$j_{\rm obs} = \frac{1}{E_2 - E_{\rm l}}\int_{E_{\rm l}}^{E_2} j(E)dE. \quad (7)$$

According to the considerations above and in Fahr & Verscharen (2016), we can approximately use $E_0 \approx 1$ keV and normalize the energies with it so that $\hat{E} = E/E_0$ and

$$j_{\rm obs} \approx \frac{1}{33\sqrt{2\pi^3}}\frac{n_e}{\sqrt{E_0 m_e}}\frac{\Gamma(\kappa+1)}{\kappa^{3/2}\Gamma(\kappa-1/2)} \times \int_{37}^{70}\hat{E}\left[1+\frac{\hat{E}}{\kappa}\right]^{-\kappa-1}d\hat{E}. \quad (8)$$

A reasonable estimate for the electron number density downstream of the termination shock located at about 90 au with a compression ratio of $s \approx 2.5$ is $n_e \approx 2.5\, n_e(1\,{\rm au})/90^2 \approx 1.5 \cdot 10^{-3}\,{\rm cm}^{-3}$. Consequently, one has

$$\frac{n_e}{\sqrt{E_0 m_e}} \approx \frac{2\cdot 10^9}{{\rm cm^2\ s\ MeV}} \quad (9)$$

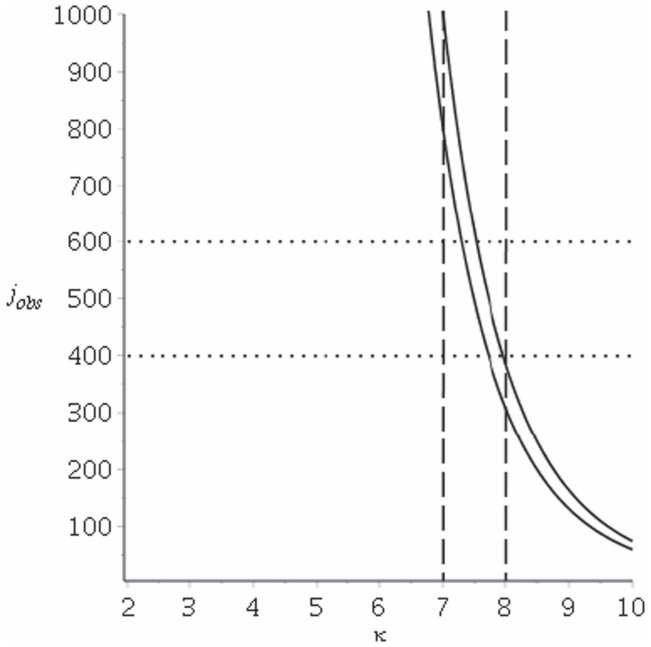


**Figure 2.** Differential flux $j_{\rm obs}$ (in units of electrons $\rm cm^{-2}\,s^{-1}\,sr^{-1}\,MeV^{-1}$) quantitatively estimated with Equation (10) as a function of $\kappa$. The lower and upper solid curves are for $E_0 = 1$ keV and $E_0 = 0.64$ keV, respectively, the latter corresponding to a 20% lower $U_\perp$ (see the discussion in Section 4).

so that

$$
\begin{aligned}
&j_{\rm obs}\,[\text{electrons cm}^{-2}\,\text{s}^{-1}\,\text{sr}^{-1}\,\text{MeV}^{-1}] \\
&\approx 7.7\cdot 10^6 \frac{\Gamma(\kappa+1)}{\kappa^{3/2}\Gamma(\kappa-1/2)}\int_{37}^{70}\hat{E}\left[1+\frac{\hat{E}}{\kappa}\right]^{-\kappa-1} d\hat{E} \\
&= 7.7\cdot 10^6 \frac{\Gamma(\kappa+1)[38(\kappa+37)^{-\kappa}-71(\kappa+70)^{-\kappa}]\,\kappa^{\kappa-1/2}}{\Gamma(\kappa-1/2)(\kappa-1)}
\end{aligned}
\tag{10}
$$

A plot of $j_{\rm obs}$ as a function of $\kappa$ is shown in Figure 2 and reveals that the measured values of 400–600 electrons $\rm cm^{-2}\,s^{-1}\,sr^{-1}\,MeV^{-1}$ (e.g., Decker et al. 2015) are reproduced with $\kappa \approx 7$ to $\kappa \approx 8$.

Given that this estimate concerns measurements that cover the entire width of the inner heliosheath along the trajectory of the *Voyager 1* spacecraft, we can conclude that the electron distribution downstream of the termination shock relaxes toward a Maxwellian with temperature $T_{e2} = m_e U_\perp^2/(3k_{\rm B})$. Note, however, that the Maxwellian limit is not reached: the limit $\kappa \to \infty$ in Equation (10) gives $j_{\rm obs} \approx 10^{-17}$ electrons $\rm cm^{-2}\,s^{-1}\,sr^{-1}\,MeV^{-1}$, i.e., a value far below the measurements.

## 4. Discussion

The above estimate reveals that already only moderately low $\kappa$-values of $7 \leqslant \kappa \leqslant 8$ are sufficient to explain the differential electron fluxes measured by *Voyager 1* in the energy interval from 37 to 70 keV. While a more rigorous hydrodynamic modeling of the evolution of the $\kappa$-parameter along heliosheath flow lines will be described in a forthcoming paper analogously to the model in Fahr et al. (2016), here we would like to draw attention to the fact that the core width $U_\perp$ of the resulting $\kappa$-distribution depends not only on the upstream solar wind bulk velocity $U_1$, but also on the angle $\alpha_1$ between the upstream magnetic field and the shock normal. Consequently, the temperature $T_{e2}$ also depends on that angle. To illustrate the effect of only a quasi-parallel or oblique shock, Figure 2 also displays the estimate for a 20% lower $U_\perp$, translating to a ∼25% higher electron flux.

In potential compensation for that, in these cases a field-aligned electron flux component $U_\parallel$ appears, representing a field-aligned electric current that may be unstable with respect to driving whistler wave turbulence, as has been discussed by Scime et al. (1994) and by Gary et al. (1994). This points to the following situation. On the one hand, if the shock is quasi-perpendicular, the downstream electron distribution function has a maximum value $\Theta(\alpha_1) = \Theta(\pi/2)$ and an associated electric current does not exist that could drive whistler waves that effectively help to convert the original halo distribution into a *kappa* distribution. On the other hand, if the shock is quasi-parallel, the value $\Theta(\alpha_1 \ll \pi/2)$ would become comparatively small and the resulting electric current would be the strongest. The possibly excited whistler waves then quickly convert the initial distribution function into a suprathermal $\kappa$-distribution due to wave–particle induced energy diffusion.

## 5. Summary and Conclusions

We have demonstrated that the suprathermal 37–40 keV electron fluxes observed by the *Voyager 1* spacecraft in the inner heliosheath are most likely of solar wind origin. The original electron distribution function is, during its passage across the solar wind termination shock, first transformed into a torus distribution and, subsequently, due to the action of wave–particle interaction-induced energy diffusion, into a suprathermal power-law distribution. Assuming that the latter can be represented by a $\kappa$-distribution, we have shown that the measured electron flux levels can be explained with moderately low $\kappa$-values between 7 and 8. While this may indicate a relaxation of the distribution toward a Maxwellian during its convection through the inner heliosheath, such values correspond to its prevailing suprathermal character.

The work of H.J.F., H.F., K.S., A.S., S.E.S.F., and M.S.P. was carried out within the framework of the bilateral BMBF-NRF-project "Astrohel" (01DG15009) funded by the German Bundesministerium für Bildung und Forschung (BMBF) and the South African National Research Foundation (NRF). The responsibility of the contents of this work is with the authors.

## ORCID iDs

H. Fichtner https://orcid.org/0000-0002-9151-5127
K. Scherer https://orcid.org/0000-0002-9530-1396
S. E. S. Ferreira https://orcid.org/0000-0001-8264-1044
M. S. Potgieter https://orcid.org/0000-0001-8615-1683

## References

Bogdan, T. J., Lee, M. A., & Schneider, P. 1991, JGR, 96, 161
Chalov, S. V., & Fahr, H. J. 2013, MNRAS, 433, L40
Decker, R. B., Krimigis, S. M., Roelof, E. C., & Hill, M. E. 2015, JPhCS, 577, 012006
Fahr, H. J., & Fichtner, H. 2011, A&A, 533, A92
Fahr, H. J., Richardson, J. D., & Verscharen, D. 2015, A&A, 579, A18
Fahr, H.-J., & Siewert, M. 2013, A&A, 558, A41
Fahr, H.-J., Sylla, A., Fichtner, H., & Scherer, K. 2016, JGRA, 121, 8203
Fahr, H. J., & Verscharen, D. 2016, A&A, 587, L1

Gary, S. P., Scime, E. E., Phillips, J. L., & Feldman, W. C. 1994, JGR, 99, 23391
Hapgood, M., Perry, C., Davies, J., & Denton, M. 2011, P&SS, 59, 618
Isenberg, P. A. 1987, JGR, 92, 1067
Krimigis, S. 2015, in New Paradigms for the Outer Heliosphere, Invited Talk, http://helio_cr.tp4.rub.de/Outer_Heliosphere/Science.php
Langner, U. W., de Jager, O. C., & Potgieter, M. S. 2001, AdSpR, 27, 517
Lembège, B., Savoini, P., Balikhin, M., Walker, S., & Krasnoselskikh, V. 2003, JGRA, 108, 1256
Prinsloo, P. 2016, M.Sc. thesis, North-West Univ. http://repository.nwu.ac.za/bitstream/handle/10394/18956/Prinsloo_PL_2016.pdf
Prinsloo, P. L., Potgieter, M. S., & Strauss, R. D. 2017, ApJ, 836, 100
Scime, E. E., Bame, S. J., Feldman, W. C., et al. 1994, JGR, 99, 23401
Stone, E. C., Cummings, A. C., McDonald, F. B., et al. 2013, Sci, 341, 150
Webber, W. R., & McDonald, F. B. 2013, GeoRL, 40, 1665
Wykes, W. J., Chapman, S. C., & Rowlands, G. 2001, PhPl, 8, 2953